Nuclear Engineering and Technology 51 (2019) 356–368

Contents lists available at ScienceDirect

Nuclear Engineering and Technology

journal homepage: www.elsevier.com/locate/net

Original Article

Verification and validation of STREAM/RAST-K for PWR analysis

Jiwon Choe [a], Sooyoung Choi [b], Peng Zhang [a], Jinsu Park [a], Wonkyeong Kim [a], Ho Cheol Shin [c], Hwan Soo Lee [c], Ji-Eun Jung [c], Deokjung Lee [a, *]

[a] Department of Nuclear Engineering, Ulsan National Institute of Science and Technology (UNIST), 50 UNIST-gil, Ulsan, 44919, Republic of Korea
[b] Research Division of Mechanical, Aerospace and Nuclear Engineering, Ulsan National Institute of Science and Technology (UNIST), 50 UNIST-gil, Ulsan, 44919, Republic of Korea
[c] Core and Fuel Analysis Group, Korea Hydro & Nuclear Power Central Research Institute (KHNP-CRI), Daejeon 34101, Republic of Korea

ARTICLE INFO

Article history:
Received 20 May 2018
Received in revised form
27 September 2018
Accepted 4 October 2018
Available online 5 October 2018

Keywords:
Verification and validation
PWR core
Two-step approach
STREAM
RAST-K 2.0

ABSTRACT

This paper presents the verification and validation (V&V) of the STREAM/RAST-K 2.0 code system for a pressurized water reactor (PWR) analysis. A lattice physics code STREAM and a nodal diffusion code RAST-K 2.0 have been developed by a computational reactor physics and experiment laboratory (CORE) of Ulsan National Institute of Science and Technology (UNIST) for an accurate two-step PWR analysis. The calculation modules of each code were already verified against various benchmark problems, whereas this paper focuses on the V&V of linked code system. Three PWR type reactor cores, OPR-1000, three-loop Westinghouse reactor core, and APR-1400, are selected as V&V target plants. This code system, for verification, is compared against the conventional code systems used for the calculations in nuclear design reports (NDRs) and validated against measured plant data. Compared parameters are as follows: critical boron concentration (CBC), axial shape index (ASI), assembly-wise power distribution, burnup distribution and peaking factors. STREAM/RAST-K 2.0 shows the RMS error of critical boron concentration within 20 ppm, and the RMS error of assembly power within 1.34% for all the cycles of all reactors.

1. Introduction

The work presented in this paper is the verification and validation (V&V) of the STREAM/RAST-K 2.0 (ST/R2) code system for the core design of pressurized water reactors (PWRs). A conventional two-step approach of a transport calculation and a nodal diffusion calculation, such as CASMO/SIMULATE (or PARCS), HELIOS (or CASMO, DeCART)/MASTER, DIT/ROCS, PARAGON (or PHOENIX)/ANC and KARMA/ASTRA [1–12], has been used in the light water reactor core design for decades and there have been many studies aiming at increasing the accuracies of reactor core analyses [13]. Those conventional code systems have been in use for commercial PWR core designs for a long time, and they have been upgraded continuously based on numerous core follow calculations. However, the conventional code systems usually adopt methodologies developed in the past [14]. A lattice physics code STREAM and a nodal diffusion code RAST-K 2.0 have been developed by a computational reactor physics and experiment laboratory (CORE) in Ulsan National Institute of Science and Technology (UNIST). Many advanced methodologies have been implemented in STREAM and RAST-K 2.0 to enhance accuracy and performance [15]. ST/R2 has been developed to be a multi-scale, multi-physics analysis code system, thus ST/R2 can be a platform in terms of neutronics code for coupling with thermal/hydraulic (TH) code and fuel performance (FP) code [16].

Solvers and features in STREAM and RAST-K 2.0 have been verified against various benchmark problems independently [13–21]. STORA has been developed as a linkage code from STREAM to RAST-K 2.0. This paper carries out comprehensive analyses on V&V of PWR modeling of RAST-K 2.0 using a cross section library generated by STREAM. The reactor cores of three PWR types, OPR-1000, three-loop Westinghouse nuclear power plant (NPP), and APR-1400, have been modelled and analyzed, and a total of 24 cycles for five NPP units were simulated by ST/R2. This code system is verified by comparing against conventional code systems used for the calculations of nuclear design reports (NDR) and validated against plant measured operation data. Compared parameters are as follows: critical boron concentration (CBC), axial shape index

* Corresponding author.
E-mail addresses: chi91023@unist.ac.kr (J. Choe), schoi@unist.ac.kr (S. Choi), zhangpeng@unist.ac.kr (P. Zhang), jinsu@unist.ac.kr (J. Park), poryor@unist.ac.kr (W. Kim), shin.hocheol@khnp.co.kr (H.C. Shin), leehwansoo1@khnp.co.kr (H.S. Lee), jejung10@khnp.co.kr (J.-E. Jung), deokjung@unist.ac.kr (D. Lee).

https://doi.org/10.1016/j.net.2018.10.004

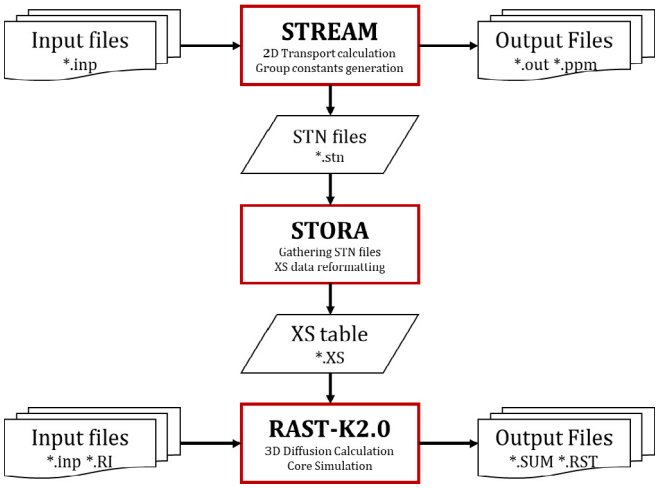

Fig. 1. Flowchart of STREAM/RAST-K 2.0 code system.

(ASI), assembly-wise power distribution, burnup distribution and peaking factors.

2. Two-step approach code system

In the ST/R2 code system, the lattice code is STREAM and the core simulator is RAST-K 2.0 as in Fig. 1. The STREAM solves neutron transport equation for two-dimensional assembly and reflector models and stores group constants, number density and form function in STN (STREAM To Nodal code) file. The STORA binds all STN files and reformat them as one XS (Cross Section) file. The RAST-K 2.0 simulates three-dimensional core calculation with the XS file.

2.1. STREAM

STREAM (Steady state and Transient REactor Analysis with Method of characteristics) uses the method of characteristics (MOC) for transport calculation and it adopts both a pin-based pointwise energy slowing-down method (PSM) and the equivalence theory for resonance treatment [17]. An embedded depletion module is available using the Chebyshev Rational Approximation Method (CRAM) [18]. Engineering features are implemented to support convenient PWR modeling, such as automatic thermal expansion, few-group constant generation for nodal code, subchannel TH calculation, and source term calculation. STREAM was verified through 26 benchmark problems [19] [20]. For the fuel assemblies (FAs) in the VERA benchmark, STREAM shows high accuracy within ±100 pcm differences in k_{eff} and ±0.1% differences in pin power distribution compared to the Monte Carlo code results [20]. It also displays these results in order of ±100 pcm difference in k_{eff} compared to the Monte Carlo solution of assembly depletion problems, such as 17×17 FA with 3.1 wt% enriched UO_2 fuel and 17×17 FA with 24 gadolina pins [20]. STREAM can analyze PWR fuel pin-cell problems, two-dimensional (2D) cores, three-dimensional (3D) cores, and spent fuel problems [21]. Table 1 summarizes the comparison of code features of conventional lattice codes and STREAM.

STREAM generates multi-group constants and homogenized cross section data through 2D FA calculation. The case matrices at hot state for FAs and reflectors are summarized in Table 2 and Table 3. Full case matrices to consider not only steady state, but also transient simulation, are shown in Fig. 2 and Fig. 3. This paper contains V&V results for normal operation, thus only a hot state case matrix is used for the branch calculation in STREAM. Users can control the case matrix, such as moderator temperature range or

Table 2
Case matrix for FAs for hot steady state.

Reference		Burnup [GWd/MT]	0–80		
Branch	1	Boron [ppm]	0.1	Boron *2	2400
	2	$T_{Moderator}$ [K]	$T_{Moderator}$ −20	$T_{Moderator}$ +20	
	3	Boron [ppm]	0.1	Boron *2	2400
		$T_{Moderator}$ [K]	$T_{Moderator}$ −20	$T_{Moderator}$ +20	
	4	$T_{Moderator}$ [K]	$T_{Moderator}$ −20		
		T_{Fuel} [K]	$T_{Moderator}$ −20	1500	
	5	$T_{Moderator}$ [K] Control Rod	$T_{Moderator}$ −20 Inserted	$T_{Moderator}$ +20	
	6	$T_{Moderator}$ Detector	$T_{Moderator}$ −20 Inserted	$T_{Moderator}$+20	

Table 1
Comparison of conventional lattice codes and STREAM.

	Conventional Lattice Codes	STREAM
Resonance self-shielding calculation for fuel	Subgroup and/or Equivalence theory - Complicated library generation system - Long calculation time for XS calculation - Inaccurate resonance interference model, resonance - Scattering source model - Empirical correction on XS	PSM and/or Equivalence theory + Simple procedure for library generation + Fast resonance treatment calculation + Accurate resonance interference model, resonance scattering source model + No empirical correction
Resonance treatment of ring-type material	Ignored or use of typical XS - Limited accuracy	Explicit treatment (cladding, BP) + High accuracy
Depletion	~300 nuclides - Limited applications	~1600 nuclides + Applicable to design new fuel & BP + Applicable to spent fuel analysis
Energy release per fission model	Constant kappa model - Use of typical value of energy per fission	On-the-fly kappa model + Problem-dependent
Transport correction	Outflow transport correction - Limited accuracy for high leakage problem	Inflow transport correction + Accurate
Critical spectrum calculation	B_1, P_1 - Limited accuracy	CASMO-4E method + Accurate
3D transport calculation	2D-MOC/1D-SP3 + Fast calculation time - Instability issues	Hybrid 2D/3D MOCDD - Slower than 2D/1D calculation + Stable convergence behavior

+ is Pros, and - is Cons.

Table 3
Case matrix for reflectors for hot steady state.

Reference		Burnup [GWd/MT]	0		
Branch	1	T Moderator [K]	T Moderator −20	T Moderator +20	
	2	Boron [ppm]	0.1	Boron *2	2400
		T Moderator [K]	T Moderator −20	T Moderator +20	

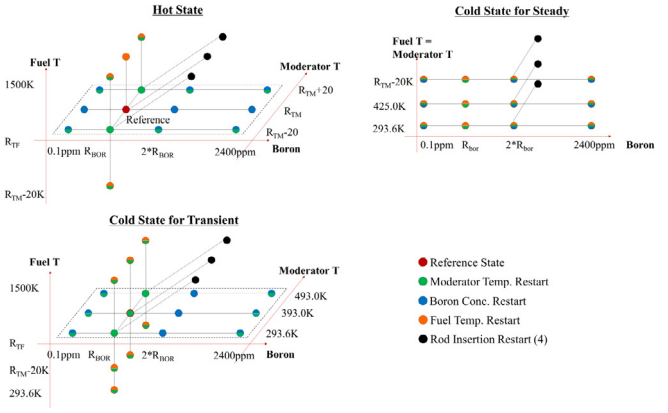

Fig. 2. FA case matrix model without burnup dependence for all states.

maximum fuel temperature, to cover transient simulation. Fundamental mode calculation and critical spectrum calculation are performed for the generation of FA 2G constants. RAST-K 2.0 does not calculate the spacer grid explicitly, thus the spacer grid material is smeared in the coolant of the active fuel region when modeling the assemblies in STREAM.

2.2. STORA

STORA (STREAM TO RAST-K 2.0) is a linking code which processes STREAM STN files into a XS file for use in RAST-K 2.0. The code reads the following data from STN files:

- State points: burnup, fuel temperature, moderator temperature, boron concentration, control rod position
- 2-group assembly/corner discontinuity factors
- 1-group power distribution (gamma smeared power distribution)
- 1-group fission and power distribution (power without gamma smearing)
- 1-group xenon and samarium chain data
- 2-group macroscopic cross section, Σ_{tr}^{2g}, Σ_{a}^{2g}, Σ_{r}^{2g}, Σ_{f}^{2g}, $\nu\Sigma_{f}^{2g}$, $\kappa\Sigma_{f}^{2g}$
- Number density, σ_{tr}^{2g}, σ_{a}^{2g}, σ_{r}^{2g}, σ_{f}^{2g}, ν^{2g}, κ^{2g} for 44 isotopes
- Delayed neutron and kinetics data
- Data for detector signal reconstruction
- Decay constants and fission yield data

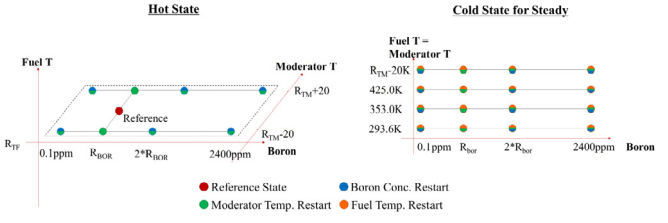

Fig. 3. Reflector case matrix model for all states.

Cross sections (or group constants) are functions of fuel temperature, moderator temperature, boron concentration, position of control rods, and burnup as follows:

$$\Sigma(S_g, BU_g) = \Sigma_b(S_b, BU_g) + d\Sigma(S_g, BU_g) \quad (1)$$

where S is the state point ($\sqrt{T_{fuel}}$, $T_{coolant}$, Boron Conc., Position of Control Rod), BU is the burnup point, Σ is any kind of cross section, Σ_b is the base cross section, S_b is the base state point, $d\Sigma$ is the deviation of cross section from the base state, and g is the given state. Cross section is interpolated separately from S and BU. The state point dependent cross section model and the burnup dependent cross section model are shown in Figs. 2 and 4, respectively.

The base state burnup calculations are done with a fine burnup grid, while the restart calculations are done only at some selected burnup steps, i.e., the branch calculations are based on a coarse burnup grid. Therefore, the base state cross sections are given on a fine burnup grid, while the cross sections for the branch states are given on a coarse grid. Σ_b and $d\Sigma$ of Eq. (1) can be described as follows:

$$\Sigma_b(S_b, BU_g) = c_i\Sigma_b(S_b, BU_i) + c_j\Sigma_b(S_b, BU_j), \quad (2)$$

$$\begin{aligned} d\Sigma(S_g, BU_g) &= c_x d\Sigma(S_g, BU_x) + c_y d\Sigma(S_g, BU_y) \\ &= c_x \sum_{a=1}^{N} w_a \Sigma(S_a, BU_x) + c_y \sum_{a=1}^{N} w_a \Sigma(S_a, BU_y), \end{aligned} \quad (3)$$

where c is the interpolation factor, i and j are fine burnup points, x and y are coarse burnup points, w is the weighting factor of each branch, and N is the number of branches cases.

2.3. RAST-K 2.0

RAST-K 2.0 utilizes the non-linear scheme based on multi group coarse mesh finite difference (CMFD) acceleration with the 3D multi group unified nodal method (UNM) to perform both steady state and transient calculations [22]. The UNM nodal solver can select any of the available diffusion analysis methods by choosing the nodal basis functions. RAST-K 2.0 has both macroscopic depletion and microscopic depletion modules. CRAM is adopted in the microscopic depletion modules for heavy nuclide chain and fission product chain as in Fig. 5 and Fig. 6 [18]. The effective Gd isotope depletion model is implemented for the accuracy in treating strong Gd spatial self-shielding effect [23] [24]. It is possible to track the amount of each main nuclide one by one to consider the history effect [25]. The simplified 1D single channel TH (TH1D) solver of nTRACER has been ported into RAST-K 2.0 for the TH feedback on cross section correction [26]. An average fuel pin is selected in each node and both moderator temperature and fuel temperature are updated axially through TH feedback calculations done by the TH1D solver. This code also provides computation modules for modeling commercial PWRs

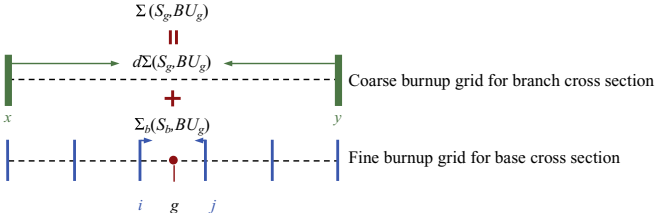

Fig. 4. The burnup dependent cross section model for FA.

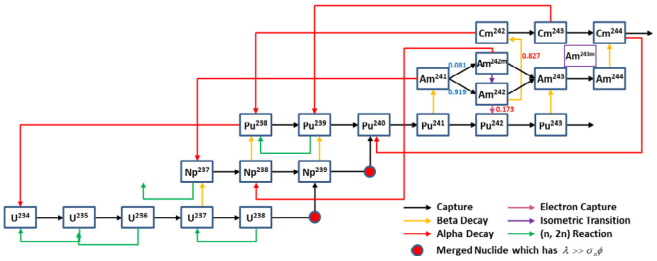

Fig. 5. Burnup chain of heavy nuclides.

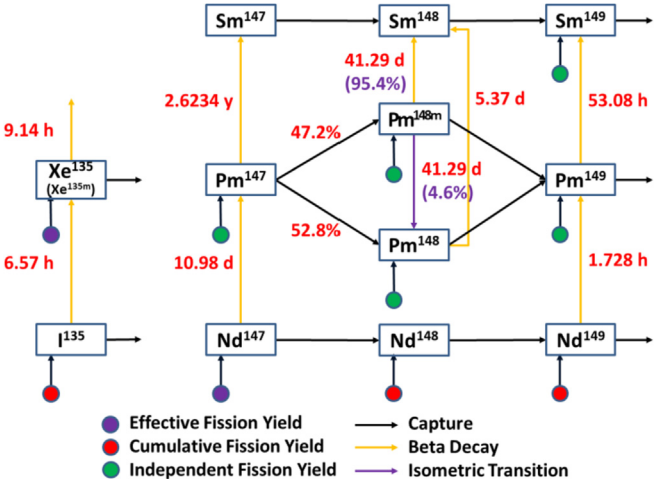

Fig. 6. Burnup chain of fission products.

such as pin power reconstruction, explicit equilibrium/transient depletion calculation for Xe & Sm chains, restart capability, branch calculation, FA shuffling and rotation, in-core/ex-core detector signal generation, N-1 cycle jump-in modeling and a simple crud prediction model. Table 4 compares RAST-K 2.0 with conventional diffusion nodal codes [25].

3. Benchmark problems for verification and validation

3.1. Reactor cores for benchmark problems

ST/R2 simulated three reactor types of five NPP units with 24 cycles. OPR-1000 and APR-1400 are two-loop PWRs designed by the Republic of Korea, and Westinghouse three-loop (WH3L) is a three-loop PWR designed by Westinghouse as shown in Fig. 7. A common design feature of these three reactor types is the three-batch reloading scheme with fresh/once burned/twice burned FAs. This paper analyzes the operation of the cores within the past 15 years, and thus only gadolinia is used as a burnable absorber material for all reactor types in this paper.

There is either an axial cutback and an axial blanket region depending on the fuel types. The OPR-1000 core consists of 177 FAs of a 16×16 array of 236 fuel rods and 5 guide tubes as in Fig. 8 (A). The WH3L core consists of 157 FAs of a 17×17 array of 264 fuel rods and 24 guide thimbles as in Fig. 8 (B). The APR-1400 core consists of 241 FAs, same as the ones of OPR-1000 in Fig. 8 (A).

The fuel material utilized is urania (UO_2) and ^{235}U enrichment ranges from 1.7 to 4.7 wt%. The common burnable absorber material is gadolinia (Gd_2O_3) admixed in urania with 0.71–2.6 wt% ^{235}U enrichment. The range of gadolinia content in Gd_2O_3-UO_2 is from 6.0 to 8.0 wt%.

Table 4
Comparison of conventional nodal diffusion codes and RAST-K 2.0.

	Conventional Nodal Diffusion Codes	RAST-K 2.0
Diffusion Equation Solver	NEM, ANM, SANM, AFEN. - Each diffusion method has pros and cons depending on reactor type.	UNM (Unified Nodal Method) + NEM/ANM/AFEN kernels can be selected as needed.
Depletion Calculation	Macro- or Micro- depletion (Analytic solution by linearization of depletion chain) + Rapid calculation time. - Limitation of number of depletion isotopes for decay chain linearization. - Limited number of heavy nuclides and Gd.	Micro depletion with CRAM - Slightly slower calculation speed due to micro-depletion + Converged well with long burnup time step. + Capability to handle the depletion of new burnable absorber material
Control Rod Simulation	4/12 Finger Type, Full/Part Strength - Limited control rod scenario can be simulated.	4/12 Finger Type, Various Types of Control Rod + It can be simulated with various absorber material, tip part, axial configuration, moving direction.
Crud Model	- N/A	+ Simple crud modeling + ASI search module

+ is Pros, and - is Cons.

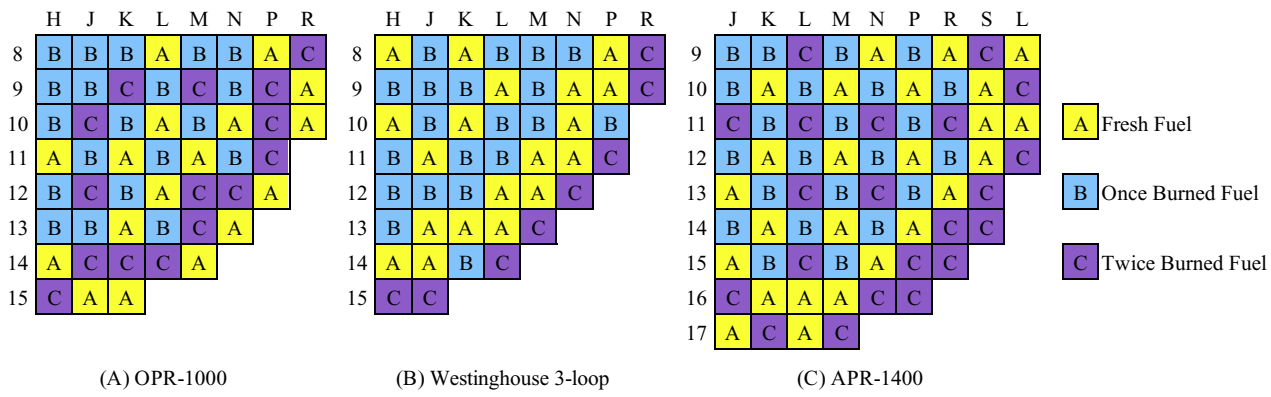

(A) OPR-1000 (B) Westinghouse 3-loop (C) APR-1400

Fig. 7. Typical loading pattern of three reactor types.

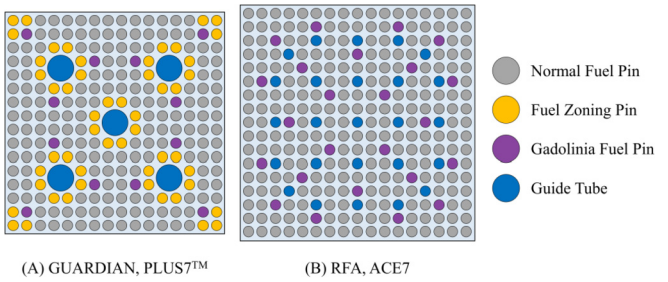

Fig. 8. Typical assembly patterns.

The result of 14 cycles among all the cycles in Table 5 are compared with measured data and NDR data. The NDR data and measured data are used for verification and validation, respectively. The compared parameters for V&V are as follows: CBC, ASI, assembly-wise power distribution, assembly-wise burnup distribution, and peaking factors (a three-dimensional power peaking factor, Fq, Maximum two-dimensional power peaking factor, Fxy, and enthalpy rise hot channel factor, F-delta-H (FΔH)). A synthesis of some measured data, such as power distribution, burnup distribution, and peaking factors, is conducted by either CECOR code or INCORE code. This study compares the boron concentration between measured, NDR, and RAST-K 2.0 data, without considering the effects of B-10 depletion. Nominal boron concentration data is available in the NDR. RAST-K 2.0 has the B-10 depletion capability as shown in Fig. 9, however in this study the nominal boron concentration results are used. True measured data reflects the effects of B-10 depletion. However, for this comparison the measured data is converted to reflect boron concentration without consideration of the effects of B-10 depletion. The NDR data is generated by DIT/ROCS, PARAGON/ANC, or PHOENIX-P/ANC.

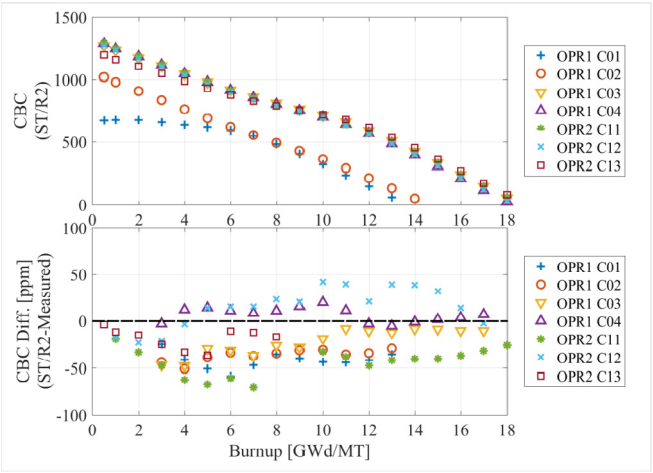

Fig. 10. Critical boron concentration difference between STREAM/RAST-K 2.0 and measured data for OPR-1000.

3.2. Calculation Options

ST/R2 uses combined ENDF/B-VII.1 and JENDL4.0 libraries for cross section and depletion libraries. The On-The-Fly kappa library

Table 5
Test model description.

Reactor Model	Reactor Power [MWth]	FA Model	Simulated Cycle[a]	Validation Cycle
OPR-1000	2815	16×16 GUARDIAN, PLUS7	OPR1 1–4 cycles OPR2 7–13 cycles	OPR1 1–4 cycles OPR2 12–13 cycles
APR-1400	3983	16×16 PLUS7	APR1 1 cycle	APR1 1 cycle
Westinghouse 3-loop	2775, 2900	17×17 RFA, ACE7	WH3L1 19–24 cycles WH3L2 19–24 cycles	WH3L1 21–24 cycles WH3L2 22–24 cycles

[a] [27–31].

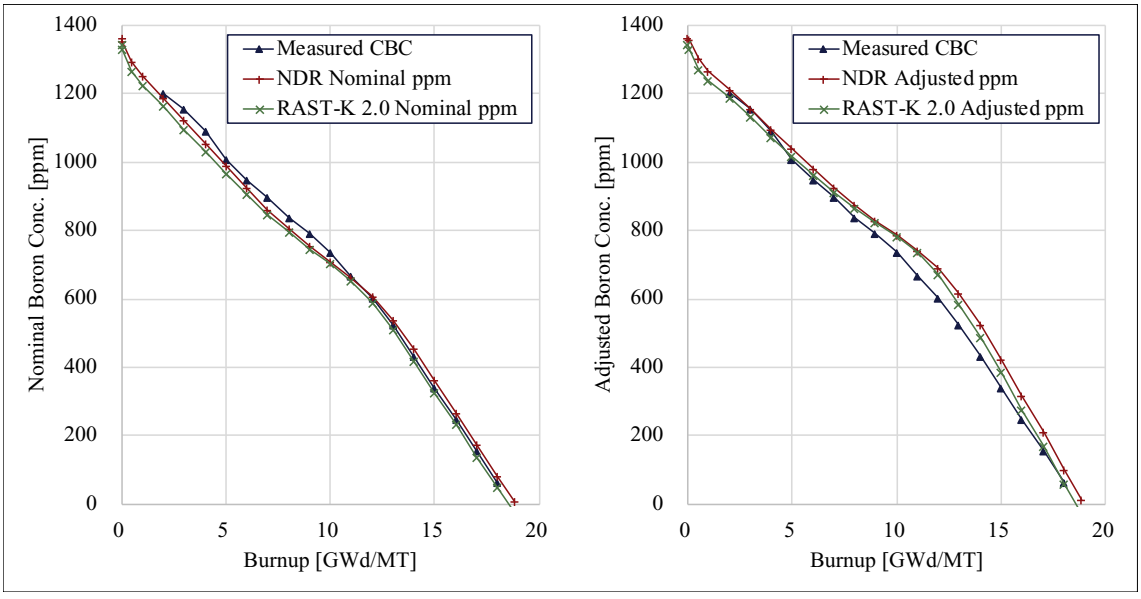

Fig. 9. Boron letdown curve comparison as effect of B-10 depletion.

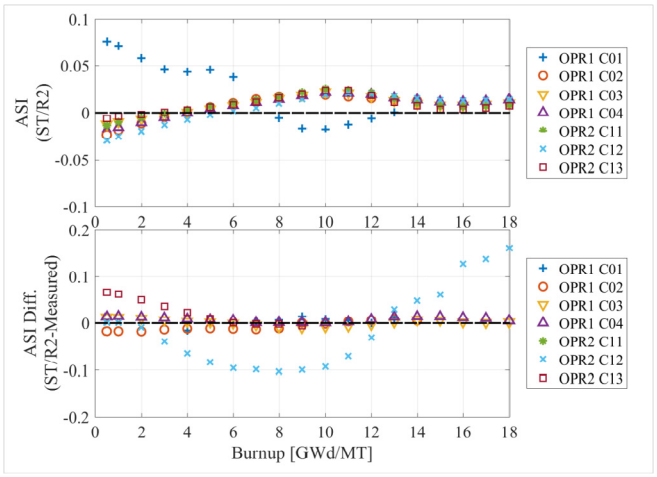

Fig. 11. Axial shape index difference between STREAM/RAST-K 2.0 and measured data for OPR-1000.

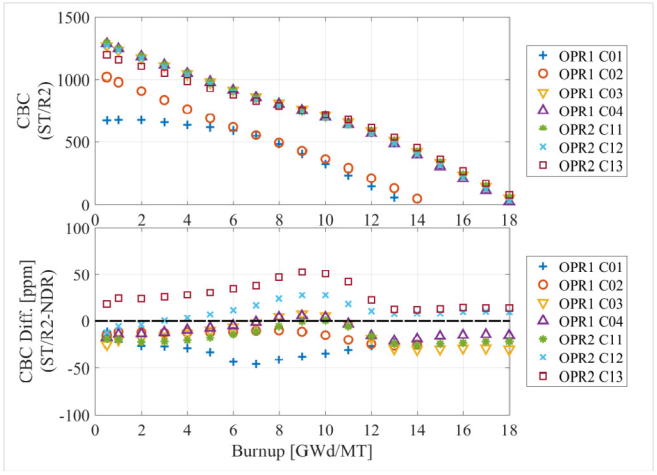

Fig. 12. Critical boron concentration difference between STREAM/RAST-K 2.0 and NDR for OPR-1000.

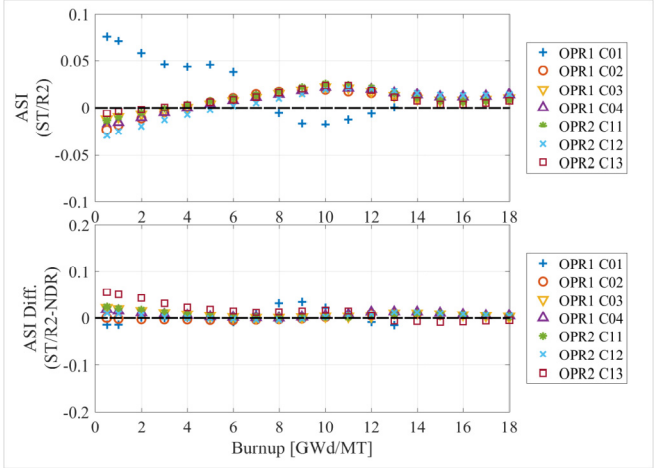

Fig. 13. Axial shape index difference between STREAM/RAST-K 2.0 and NDR for OPR-1000.

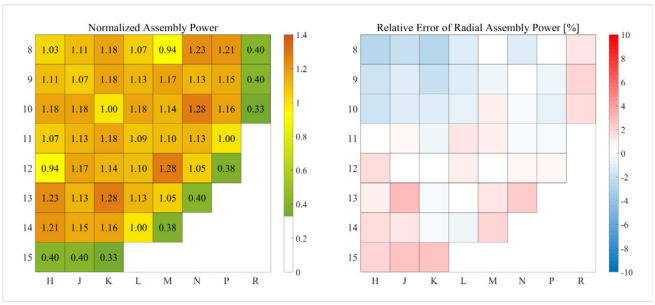

Fig. 14. Radial assembly power distribution of STREAM/RAST-K 2.0 and relative error against measured data at OPR1 C4 BOC (0.0 GWd/MT).

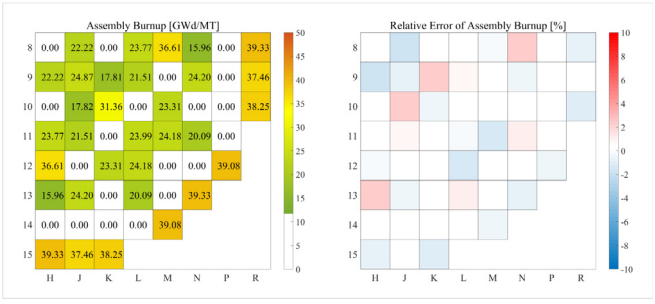

Fig. 15. Radial assembly burnup distribution of STREAM/RAST-K 2.0 and relative error against measured data at OPR1 C4 BOC (0.0 GWd/MT).

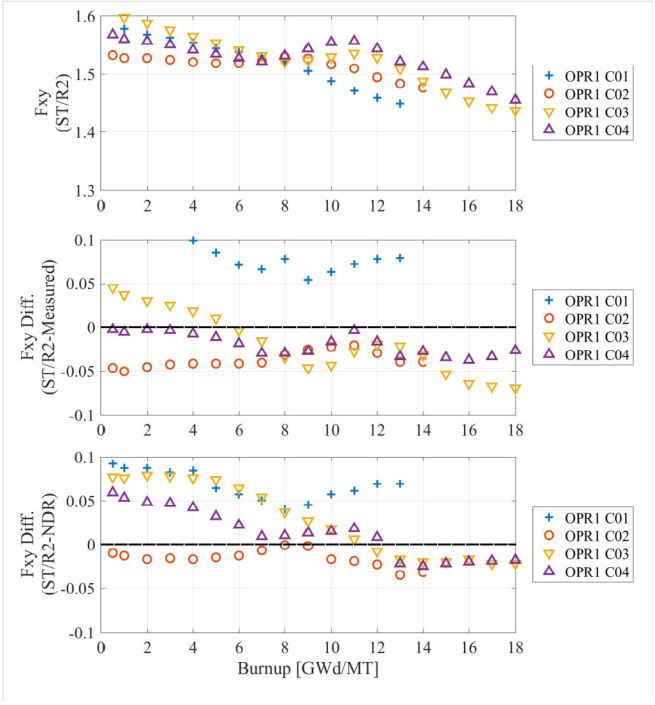

Fig. 16. Fxy results for OPR-1000.

is also used for depletion calculation in STREAM [32]. If the test model starts from an intermediate cycle, e.g., OPR2, WH3L1 and WH3L2, then RAST-K 2.0 uses the jump-in method which interpolates the number densities of 44 isotopes at a given assembly burnup from the XS file.

The STREAM uses the 72-G cross section library for transport

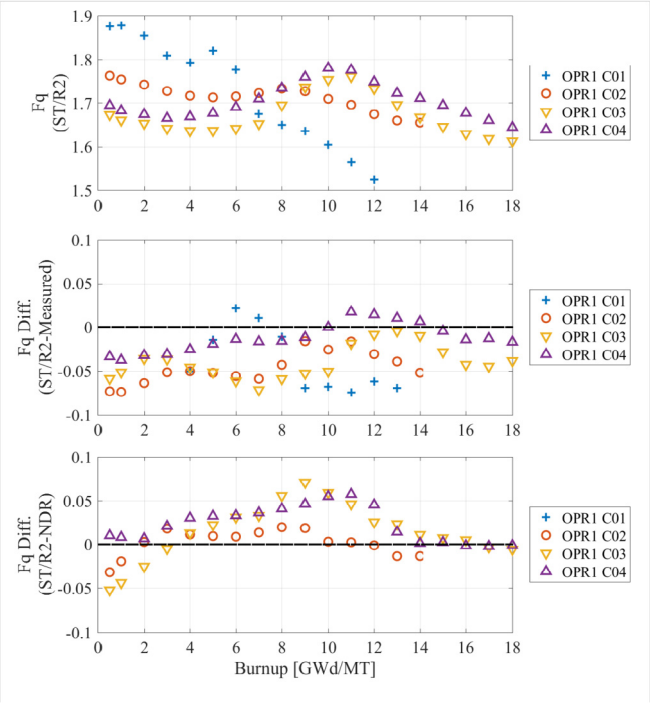

Fig. 17. Fq results for OPR-1000.

calculation, and all assemblies use the same ray condition, which is a ray spacing of 0.05 cm, 48 azimuthal and 3 polar angles. The depletion calculation of STREAM adopts a semi predictor/corrector technique and a quadratic depletion for the Gd isotopes because of the strong spatial self-shielding effect [33]. ^{238}U resonance elastic upscattering approximation is chosen in the calculations [34]. For depletion calculation, UO_2 pins and gadolinia pins are divided into 3 and 10 rings, respectively. Critical spectrum calculation is conducted during FA calculation only, and not during reflector calculation. The STREAM performs the thermal expansions, so geometry and material density are automatically adjusted according to the given temperature. Assembly discontinuity factor (ADF) is calculated with the homogenous ADF method and the radial reflector discontinuity factor preserves fuel/reflector homogenized flux ratios [35].

RAST-K 2.0 simulates 3D quarter core and performs CBC search. The predictor/corrector technique was adopted in the depletion calculation in RAST-K 2.0. Equilibrium Xe and transient Sm are calculated for each burnup point. TH feedback is also included in such a way that fuel thermal conductivity and ZrO_2 generation effects are adjusted as a function of burnup [36,37]. FAs are divided into 2×2 sub-assemblies for nodal calculation, and the number of axial nodes is 24–46 depending on the reactor core model. Both baffle and barrel geometries are considered when group constants of radial reflectors are generated.

4. Verification and validation results

4.1. OPR-1000

The OPR-1000 core consists of 177 FAs. Compared to the measured data, the CBC difference and ASI difference are smaller than 75 ppm and 0.1, respectively (Fig. 10 and Fig. 11). The ASI difference at OPR2 cycle 12 is bigger than the other cycles due to the occurrence of an axial offset anomaly (AOA) in OPR2 cycle 12. The CBC difference and ASI difference between ST/R2 and NDR are smaller than 50 ppm and 0.05 for all the cycles as shown in Fig. 12 and Fig. 13. The ASI difference at OPR2 cycle 13 between ST/R2 and NDR is bigger than the other cycles, because the NDR of OPR2 cycle 13 is calculated after the core follow calculation of the previous cycle 12, which includes the crud deposition at the top of the core.

A radial distribution of assembly power and assembly burnup is presented in Fig. 14 and Fig. 15, respectively. The result is OPR1 cycle 4 at 0.0 GWd/MT. Predictions for the assembly power of ST/R2 are 2.0% higher than the measured data at the periphery of the core. Predictions for the assembly burnup of ST/R2 are 2.0% higher for once burned FAs and 1.5% lower for twice burned FAs compared to the measured data. Peaking factors, Fxy and Fq, are presented in Fig. 16 and Fig. 17, respectively. RMS differences of peaking factors are within 0.028 compared to measured data. Table 6 summarizes V&V results of CBC, ASI, assembly power, assembly burnup and peaking factors for all the OPR-1000 core simulations. The RMS error of the assembly power and assembly burnup distributions are smaller than 1.35%.

4.2. Westinghouse three-loop plants

The WH3L core consists of 157 FAs. Compared to the measured data, the CBC difference and ASI difference are smaller than 50 ppm and 0.03, respectively (Fig. 18 and Fig. 19). Compared to NDR data, the CBC difference and the ASI difference are smaller than 50 ppm and 0.03, respectively (Fig. 20 and Fig. 21).

A radial distribution of assembly power is shown in Fig. 22. The result is from the WH3L2 cycle 22 at 0.0 GWd/MT. Assembly power of ST/R2 predictions are slightly lower than the measured data at the core center. Peaking factors, FΔH and Fq, are presented in Fig. 23 and Fig. 24, respectively. ST/R2 underestimates Fq about −0.20 compared to the measured data. The RMS difference of FΔH is around 0.033. Table 7 summarizes the V&V results of CBC, ASI, assembly power, assembly burnup and peaking factors for all the WH3L core simulations. The RMS errors of assembly power and assembly burnup results are smaller than 1.05% overall. ASI

Table 6
STREAM/RAST-K 2.0 V&V error statistics for OPR-1000.

Ref.	CBC Diff. [ppm][b]		ASI Diff. [−][b]		Assembly Power Rel. Err. [%][c]		Assembly Burnup Rel. Err. [%][c]		Fxy Diff. [−][b]		Fq Diff. [−][b]	
	NDR	M[a]	NDR	M[a]	NDR	M[a]	NDR	M[a]	NDR	M[a]	NDR	M[a]
Mean	−11.28	−5.03	0.001	0.006	0.17	0.22	0.12	−0.09	0.010	−0.004	0.005	−0.014
STD	7.89	4.94	0.029	0.006	0.16	0.28	0.26	0.30	0.018	0.017	0.013	0.013
Max.	41.83	52.74	0.161	0.056	7.04	5.42	7.56	6.52	0.092	0.099	0.071	0.021
Min.	−70.61	−46.11	−0.104	−0.016	−3.89	−3.12	−4.28	−5.08	−0.035	−0.070	−0.052	−0.075
RMS	25.15	19.45	0.032	0.012	1.35	1.34	1.14	1.27	0.030	0.028	0.017	0.027

[a] Measured.
[b] ST/R2-NDR (or Measured).
[c] (ST/R2-NDR (or Measured))/NDR (or Measured)) × 100.

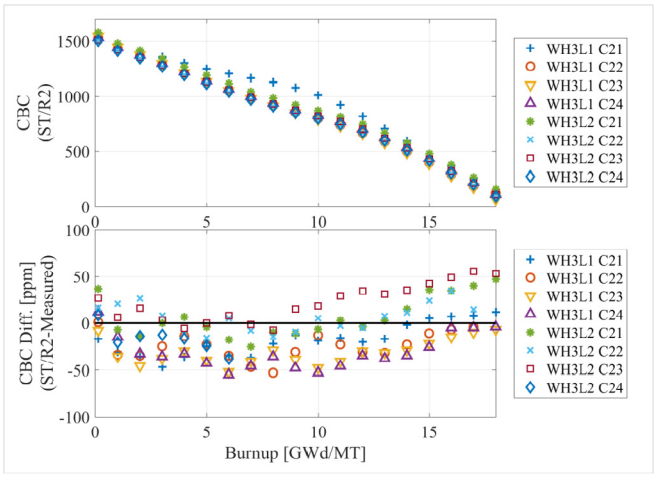

Fig. 18. Critical boron concentration difference between STREAM/RAST-K 2.0 and measured data for WH3L.

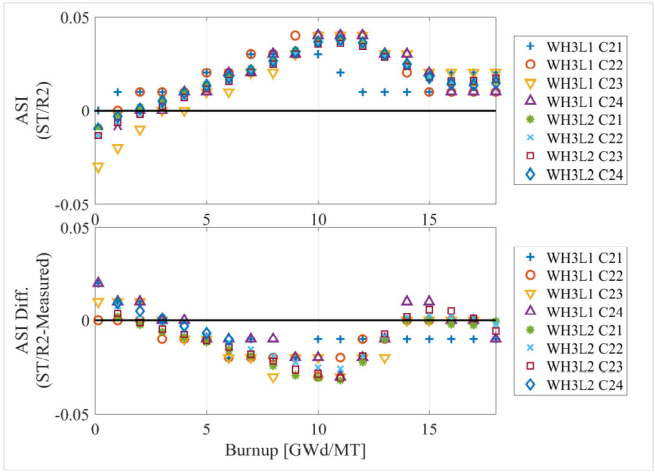

Fig. 19. Axial shape index difference between STREAM/RAST-K 2.0 and measured data for WH3L.

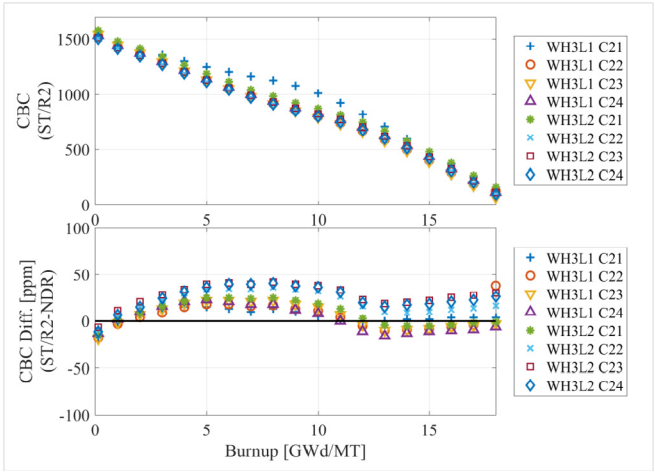

Fig. 20. Critical boron concentration difference between STREAM/RAST-K 2.0 and NDR for WH3L.

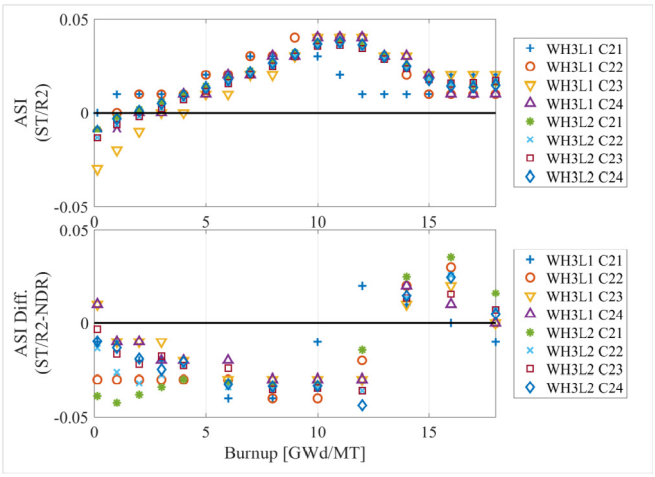

Fig. 21. Axial shape index difference between STREAM/RAST-K 2.0 and NDR for WH3L.

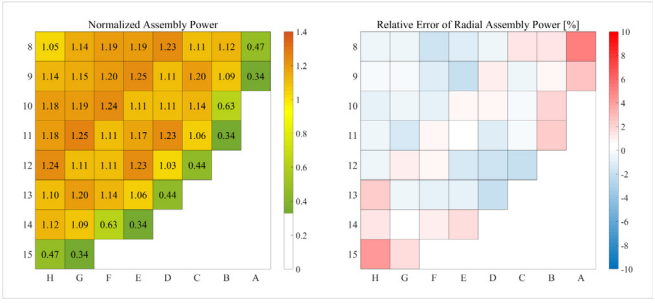

Fig. 22. Radial assembly power distribution of STREAM/RAST-K 2.0 and relative error against measured data at WH3L2 C22 BOC (0.0 GWd/MT).

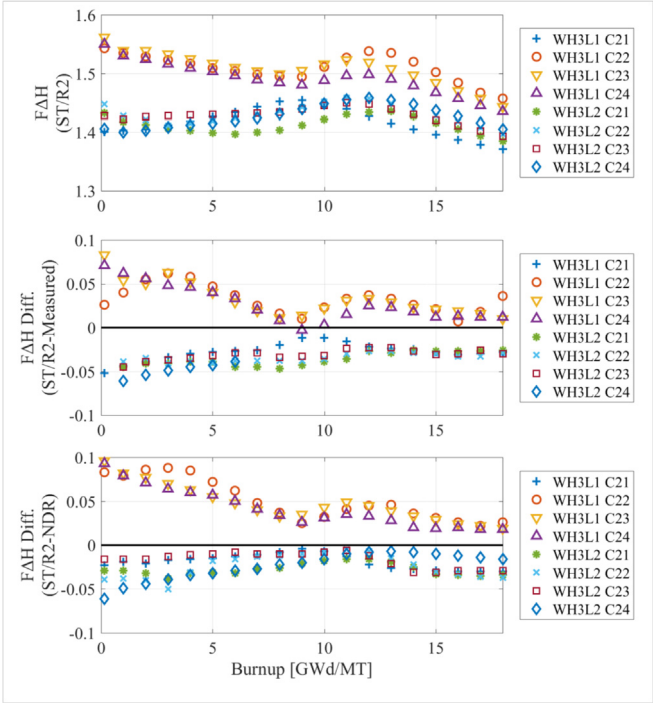

Fig. 23. FΔH results for WH3L.

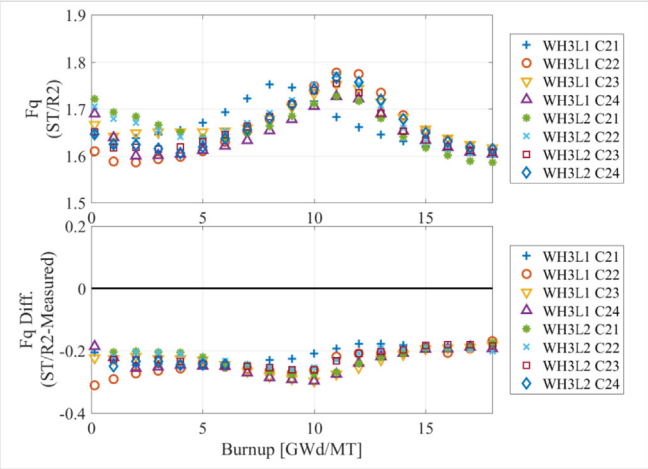

Fig. 24. Fq results for WH3L.

difference has a tendency as a function of burnup. The slope from 0 to 10 GWd/MT of measured data is steeper than that of ST/R2 as shown in Fig. 19.

4.3. APR-1400

The APR-1400 core consists of 241 FAs. The APR1 simulation was performed only for cycle 1 and for two reactor states: low power physic test (LPPT) with a nominal temperature nominal pressure (NTNP) state at BOC HZP and steady state depletions at HFP condition. The first simulation is the NTNP test at 291.3 °C and 155.1 bar. A Monte-Carlo code, MCS, and four other core design codes (PARAGON/ANC, DIT/ROCS, CMS5, and ST/R2) are used for code-to-code comparisons [38]. The core geometry is expanded to a full core for the NTNP calculation. Four tests are conducted: critical boron concentration, isothermal temperature coefficient, individual control element assembly (CEA) group worth and inverse boron worth. The location of the control rods is shown in Fig. 25. There are

Table 7
STREAM/RAST-K 2.0 V&V error statistics for WH3L.

Ref.	CBC Diff. [ppm][b]		ASI Diff. [−][b]		Assembly Power Rel. Err. [%][c]		Assembly Burnup Rel. Err. [%][c]		FΔH Diff. [−][b]		Fq Diff. [−][b]	
	NDR	M[a]	NDR	M[a]	NDR	M[a]	NDR	M[a]	NDR	M[a]	NDR	M[a]
Mean	−9.44	12.52	−0.007	−0.010	0.07	0.10	−0.10	–	0.004	−0.006	–	−0.204
STD	3.50	2.01	0.003	0.003	0.20	0.22	0.22	–	0.007	0.006	–	0.028
Max.	55.33	41.69	0.020	0.035	4.13	5.11	6.63	–	0.096	0.083	–	0.000
Min.	−55.00	−19.00	−0.032	−0.044	−2.88	−5.50	−2.70	–	−0.061	−0.061	–	−0.311
RMS	26.26	19.88	0.013	0.020	0.86	1.05	0.53	–	0.038	0.033	–	0.218

[a] Measured.
[b] ST/R2-NDR (or Measured).
[c] (ST/R2-NDR (or Measured))/NDR (or Measured)) × 100.

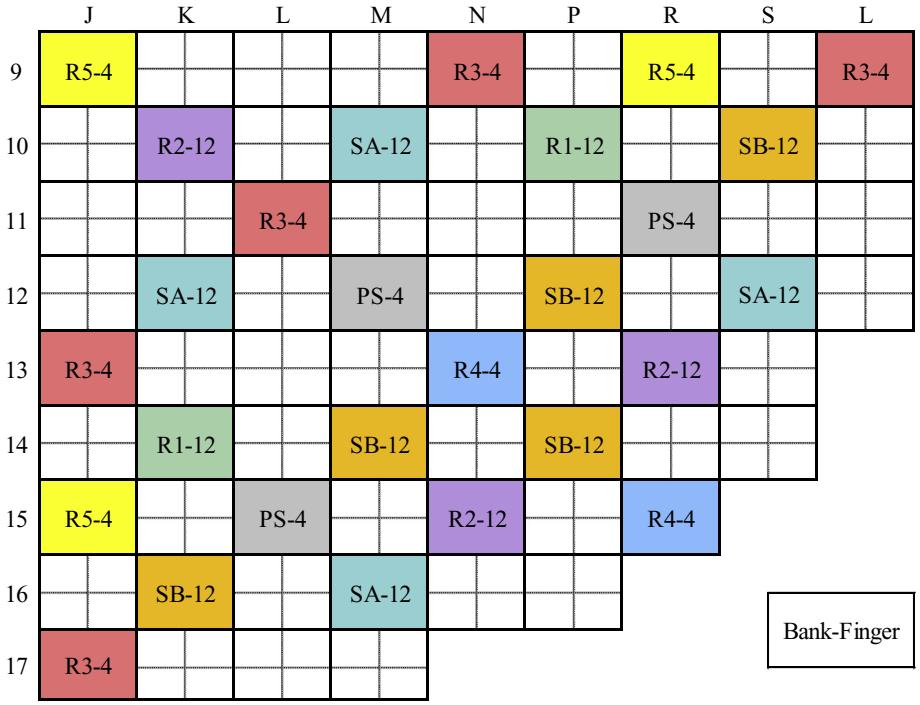

Fig. 25. Control rods location of APR1.

Table 8
Critical boron concentration [ppm].

	MCS	ST/R2		DIT/ROCS		CMS5		PARAGON/ANC	
	CBC	CBC	Diff.	CBC	Diff.	CBC	Diff.	CBC	Diff.
ARO	1186 ± 1	1150	−36	1195	9	1173	−13	1170	−16
Group 5 at 190.5 cm Withdrawn	1174 ± 1	1140	−34	1185	11	1163	−12	1160	−14
Group 5 IN	1160 ± 1	1127	−33	1173	13	1150	−10	1146	−14
Groups 5 + 4 IN	1123 ± 1	1089	−34	1134	11	1115	−8	1112	−11
Groups 5 + 4+3 IN	1063 ± 1	1031	−32	1076	13	1056	−7	1053	−10
Groups 5 + 4+3 + 2 IN	982 ± 1	948	−34	992	10	978	−4	977	−5
Groups 5 + 4+3 + 2+1 IN	871 ± 1	841	−30	892	21	867	−4	865	−6
Groups 5 + 4+3 + 2+1 + P + B + A-WRSO IN	364 ± 1	336	−28	410	46	357	−7	336	−28
Groups 5 + 4+3 + 2+1 + P + B + A IN	–	−86	–	−50	–	−38	–	−24	–

Diff. = X-MCS (X = ST/R2, DIT/ROCS, CMS5 or PARAGON/ANC).

Table 9
Isothermal temperature coefficient [pcm/°C].

	MCS	ST/R2		DIT/ROCS		CMS5		PARAGON/ANC	
	ITC	ITC	Diff.	ITC	Diff.	ITC	Diff.	ITC	Diff.
ARO	−4.00 ± 0.51	−2.27	1.73	−4.07	−0.07	−1.95	2.05	−2.67	1.33
Group 5 + 4+3 IN	−8.96 ± 0.50	−7.30	1.66	−11.24	−2.28	−9.16	−0.20	−9.32	−0.36

Diff. = X-MCS (X = ST/R2, DIT/ROCS, CMS5 or PARAGON/ANC).

Table 10
Individual CEA group worth [pcm].

Group	MCS	ST/R2		DIT/ROCS		CMS5		PARAGON/ANC	
	Worth	Worth	Diff.	Worth	Diff.	Worth	Diff.	Worth	Diff.
5 ARO	264 ± 10	255	−9	242	−22	265	1	246	−18
4 Group 5 IN	394 ± 10	412	18	425	31	408	14	365	−29
3 Groups 5 + 4 IN	667 ± 10	618	−49	628	−39	676	9	617	−50
2 Groups 5 + 4+3 IN	888 ± 11	887	−1	925	37	896	8	812	−76
1 Groups 5 + 4+3 + 2 IN	1100 ± 10	1003	−97	1054	−46	1254	154	1151	51
A Groups 5 + 4+3 + 2+1 IN	2603 ± 10	2754	151	3005	402	2890	287	2658	55
B Groups 5 + 4+3 + 2+1 + A IN	7713 ± 11	5869	−1844	7046	−667	7327	−387	6544	−1169
P Groups 5 + 4+3 + 2+1 + A + B IN	163 ± 10	122	−41	163	0	167	4	178	15

Diff. = X-MCS (X = ST/R2, DIT/ROCS, CMS5 or PARAGON/ANC).

Table 11
Inverse boron worth [ppm/pcm].

	MCS	ST/R2		DIT/ROCS		CMS5		PARAGON/ANC	
	Worth	Worth	Diff.	Worth	Diff.	Worth	Diff.	Worth	Diff.
ARO	−0.0860 ± 0.0020	−0.0755	−0.1615	−0.0924	−0.1784	−0.0900	−0.1760	−0.0928	−0.1788
Group 5 + 4+3 IN	−0.0861 ± 0.0021	−0.0786	−0.1647	−0.0921	−0.1782	−0.0896	−0.1757	−0.0927	−0.1788
Group 5 + 4+3 + 2+1 IN	−0.0883 ± 0.0020	−0.0856	−0.1739	−0.0940	−0.1823	−0.0912	−0.1795	−0.0952	−0.1835

Diff. = X-MCS (X = ST/R2, DIT/ROCS, CMS5 or PARAGON/ANC).

Table 12
Validation results of NTNP test.

Test	Group	Measured***	ST/R2	Diff.*	Err. [%]**	Acceptance Criteria***
CBC (ppm)	ARO	1163.28	1150.45	12.83	1.12	±100 ppm
ITC (pcm/°C)	ARO	−3.12	−2.27	−0.85	37.21	≤±9pcm/°C
	5 + 4+3 IN	−9.63	−7.30	−2.34	32.02	
CEA Group Worth (pcm)	5	232	255	−23	−9	±15% or ±100pcm
	4	419	412	7	2	
	3	630	618	12	2	
	2	883	887	−4	0	
	1	1143	1003	140	14	
	P	155	122	32	26	
Inverse Boron Worth (ppm/pcm)	5 + 4+3 IN	−0.093	−0.079	−0.014	18.487	±0.015 ppm/pcm

* (M − C), ** (M − C)/C*100 (M = Measured, C=ST/R2), *** [39].

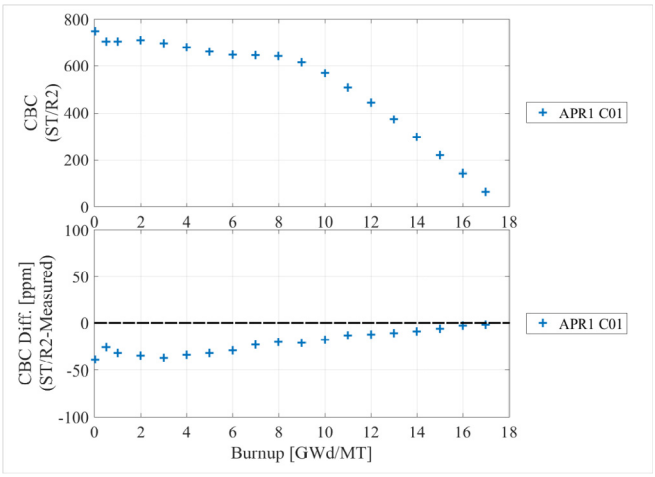

Fig. 26. Critical boron concentration difference between STREAM/RAST-K 2.0 and measured data for APR-1400.

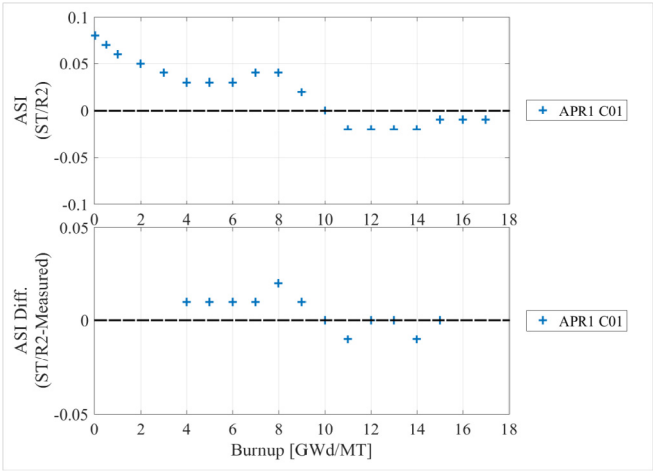

Fig. 27. Axial shape index difference between STREAM/RAST-K 2.0 and measured data for APR-1400.

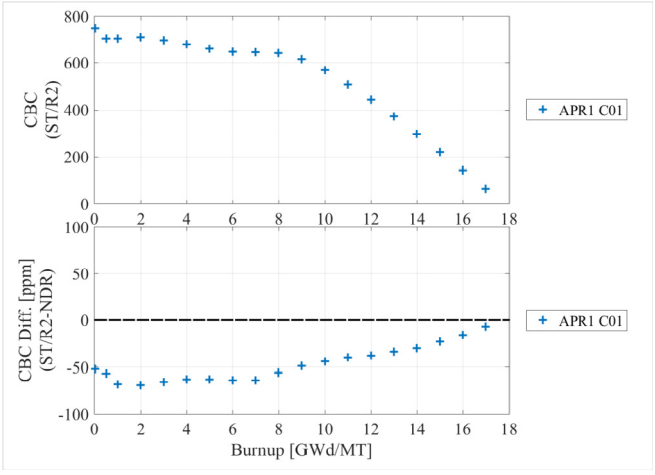

Fig. 28. Critical boron concentration difference between STREAM/RAST-K 2.0 and NDR for APR-1400.

93 control rods composed of regulating bank (R1-R5), shutdown bank (SA, SB) and part strength (PS). Regulating banks and shutdown banks use B_4C as an absorber material, and part strength uses

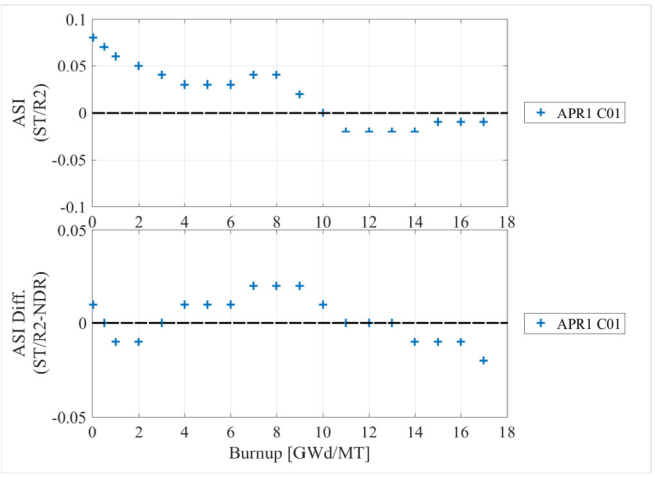

Fig. 29. Axial shape index difference between STREAM/RAST-K 2.0 and NDR for APR-1400.

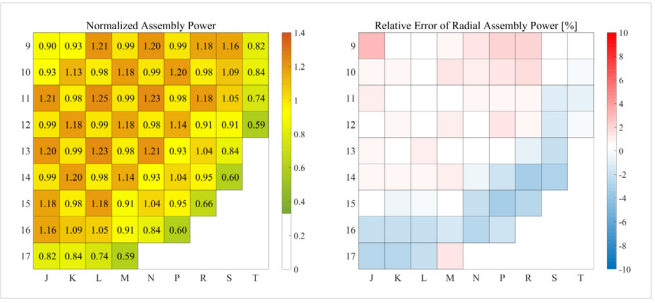

Fig. 30. Radial assembly power distribution of STREAM/RAST-K 2.0 and relative error about measured data at APR1 C1 MOC (8.0 GWd/MT).

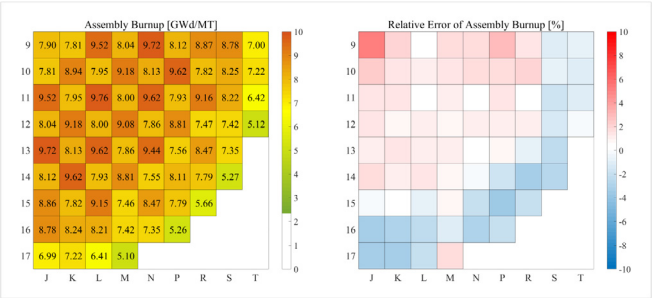

Fig. 31. Radial assembly burnup distribution of STREAM/RAST-K 2.0 and relative error about measured data at APR1 C1 MOC (8.0 GWd/MT).

Inconel to control only axial shape. The calculation results are summarized in Table 8 - Table 11.

The first test is the CBC calculation as a function of control rod insertion in Table 8. The worst rod stuck out (WRSO) is located at M-16. Overall, ST/R2 underestimates about 35 ppm compared to the MCS predictions, and 40 ppm compared to the other two-step approaches. The second test is isothermal temperature coefficient (ITC) calculation in Table 9. The temperature is perturbed by ± 5 °C in ST/R2. The ITC difference of ST/R2 is about ±2 pcm/°C compared to the results of the other codes. The third test is the individual CEA group worth calculation in Table 10. The boron concentration is fixed as a critical boron concentration at all rods out (ARO) state in Table 8, and then k_{eff} search calculation is conducted. The more control rods are inserted, the greater the rod worth difference

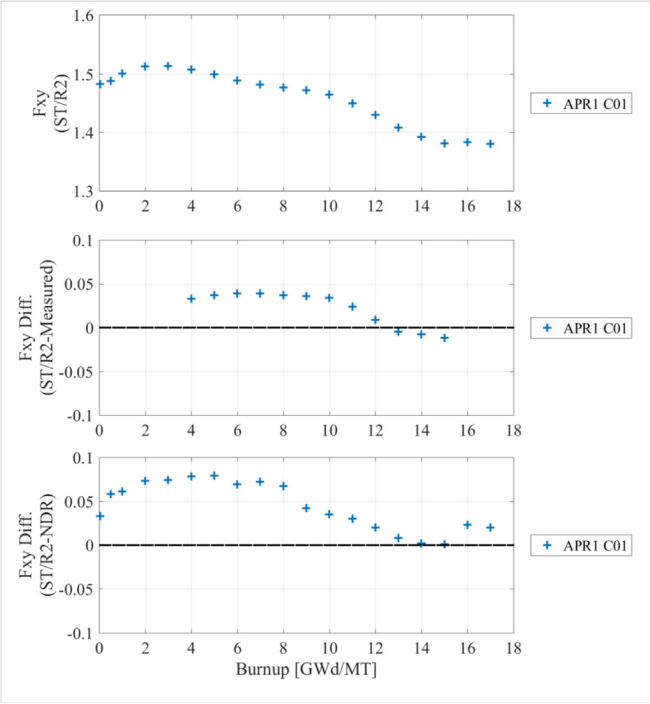

Fig. 32. Fxy results for APR-1400.

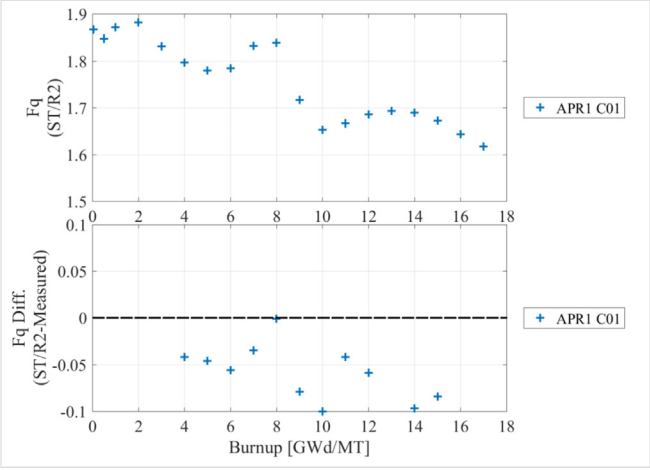

Fig. 33. Fq results for APR-1400.

between MCS and the other two-step approaches becomes. Lattice code considers the critical spectrum when generating group constants to correct neutron leakage. k_{eff} is, however, far from the criticality needed to control rod insertion, and therefore the CEA worth difference increases. In terms of relative error, it is on the order of 15% overall. The fourth test is an inverse boron worth calculation in Table 11. The difference is within 0.01 ppm/pcm, and the relative error is within 10% compared to the MCS results.

The validation results of NPNT test is summarized in Table 12 and all ST/R2 results satisfy the acceptance criteria.

The second simulation is the HFP whole core depletion calculation of APR1 cycle 1. Compared to the measured data, the CBC difference and ASI difference are smaller than 50 ppm and 0.02, respectively (Fig. 26 and Fig. 27). Compared to the NDR data, the CBC difference and the ASI difference are smaller than 70 ppm and 0.02, respectively, for all the cycles as shown in Fig. 28 and Fig. 29.

Radial distributions of assembly power and assembly burnup are presented in Fig. 30 and Fig. 31, respectively. The results are for APR1 cycle 1 to be at 8.0 GWd/MT. Both the assembly power of ST/R2 and the assembly burnup predictions are 2.0% lower than the measured data at the core periphery.

Peaking factors, Fxy and Fq, are presented in Fig. 32 and Fig. 33, respectively. Compared to the measured data, ST/R2 overestimates Fxy around 0.05 and underestimates Fq as 0.05. Both assembly power of ST/R2 and assembly burnup predictions are 2.0% lower than the measured data at the core periphery. Table 13 summarizes the V&V results of CBC, ASI, assembly power, assembly burnup and peaking factors for all the APR-1400 core simulations. The RMS error of the assembly power and that of assembly burnup are smaller than 1.50% and 1.17%, respectively.

5. Conclusion

The STREAM/RAST-K 2.0 code system of the UNIST CORE group has been verified and validated through simulations of PWR reactor cores. STREAM calculates 2D FAs and generates 2G constants. STORA combines group constant files of each FA and converts them into one cross section library file for RAST-K 2.0. RAST-K 2.0 simulates multi-cycles with 3D whole core models. Three kinds of PWR reactor types and a total of 14 cycles for five nuclear power plants were adopted for ST/R2 V&V. The RMS error of CBC of ST/R2 compared to the measured data is smaller than 20 ppm for all the cycles and ST/R2 underestimates CBC by 50 ppm at the first cycle. Other parameters compared to the measured data also show acceptable accuracy: the ASI RMS difference is 0.02, the RMS error of assembly power is 1.34% and the RMS error of assembly burnup is 1.50%. The errors of CBC of ST/R2 compared to the NDR data are smaller than 26 ppm for all cycles. Furthermore, other parameters

Table 13
STREAM/RAST-K 2.0 V&V error statistics for APR-1400.

Ref.	CBC Diff. [ppm][b]		ASI Diff. [−][b]		Assembly Power Rel. Err. [%][c]		Assembly Burnup Rel. Err. [%][c]		Fxy Diff. [−][b]		Fq Diff. [−][b]	
	NDR	M[a]	NDR	M[a]	NDR	M[a]	NDR	M[a]	NDR	M[a]	NDR	M[a]
Mean	−2.64	−5.94	0.000	0.000	0.06	−0.01	0.03	0.05	0.006	0.002	–	−0.005
STD	4.24	6.62	0.003	0.004	0.25	0.32	0.10	0.33	0.010	0.007	–	0.014
Max.	0.00	0.00	0.020	0.020	5.32	3.37	3.16	5.07	0.079	0.039	–	0.000
Min.	−39.00	−69.00	−0.010	−0.020	−2.31	−3.43	−3.26	−3.50	0.000	−0.012	–	−0.103
RMS	8.54	18.00	0.003	0.004	1.10	1.17	1.22	1.50	0.018	0.008	–	0.019

[a] Measured.
[b] ST/R2-NDR (or Measured).
[c] (ST/R2-NDR (or Measured))/NDR (or Measured)) × 100.

also provide acceptable accuracies: the RMS difference of ASI is 0.03, the RMS error of assembly power is 1.35% and the RMS error of assembly burnup is 1.22%. The RMS difference of peaking factors are less than 0.03 and LPPT results satisfy the acceptance criteria. It was successfully verified and validated that ST/R2 can provide reasonably accurate results compared to both the measured data and NDR design values without any tuning of ST/R2 physics models.

Acknowledgements

This research was supported by the project(L17S018000) by Korea Hydro & Nuclear Power Co. Ltd.. Authors would like to sincerely thank Prof. Han Gyu Joo at Seoul National University for sharing the TH1D module of nTRACER, which was crucial for the development of the STREAM/RAST-K T/H feedback module.

References

[1] SSP-09/442-U, CASMO-4E: Extended Capability CASMO-4 User's Manual, Studsvik Scandpower, 2009.
[2] SSP-09/447-U, SIMULATE-3: Advanced Three-Dimensional Two-Group Reactor Analysis Code User's Manual, Studsvik Scandpower, 2009.
[3] T. Downar, Y. Xu, V. Seker, PARCS v3.0 U.S.NRC Core Neutronics Simulator User Manual, UM-NERS-09–0001, University of Michigan, 2013.
[4] R.J.J. Stamml'er, HELIOS Methods, Studsvik Scandpower, 2002.
[5] Jin Young Cho, Jae Seung Song, Kyung Hoon Lee, Three dimensional nuclear analysis system DeCART/CHORUS/MASTER, in: ANS Annual Meeting, Atlanta, June 16–20, 2013.
[6] Chang Ho Lee, Byung Oh Cho, Jae Seung Song, Jae Seong Kim, Ha Yong Kim, Sung Quun Zee, Hyung Kook Joo, Verification of Extended Nuclide Chain of MASTER with CASMO-3 and HELIOS, KAERI/TR-947/98, Korea Atomic Energy Research Institute, 1998.
[7] R.A. Loretz, et al., User's Manual for DIT: Discrete Integral Transport Assembly Design Code, CE-CES-11 REV 4-P, April 1994.
[8] R.A. Loretz, et al., User's Manual for ROCS: Coarse and Fine Mesh Advanced Diffusion Theory Code for Reactor Core Analysis, CE-CES-4-P Rev 15, January 2003.
[9] TR-KHNP-0008, Rev. 1, Qualification of PARAGON/ANC Code System for PWR Applications, May 2007.
[10] WCAP-10965-P-A, ANC: A Westinghouse Advanced Nodal Computer Code, September 1986.
[11] T.Q. Nguyen, et al., Qualification of the PHOENIX-P/ANC Nuclear Design System for Pressurized Water Reactor Cores, WCAP-11596-P-A, June, 1988.
[12] Tae Young Han, Joo Il Yoon, Jae Hee Kim, Chang Kyu Lee, Beom Jin Cho, Benchmark verification of the KARMA/ASTRA Code with OECD/NEA and USNRC PWR MOX/UO2 transient problem, in: Proceedings of ICAPP 2011, France, 2011.
[13] Jiwon Choe, Sooyoung Choi, Minyong Park, Peng Zhang, Ho Cheol Shin, Hwan Soo Lee, Deokjung Lee, Validation of the UNIST STREAM/RAST-K Code System with OPR -1000 Multi-cycle Operation, RPHA17, Chengdu, Sichuan, China, August 24–25, 2017.
[14] Sooyoung Choi, Jiwon Choe, Jaerim Jang, Deokjung Lee, Extension of PSM for Ring-type Burnable Absorber Containing Resonant Nuclides, RPHA17, Chengdu, Sichuan, China, August 24–25, 2017.
[15] Sooyung Choi, Minyong Park, Youqi Zheng, Chidong Kong, Jiwon Choe, Hanjoo Kim, Kiho Kim, Ho Cheol Shin, Deokjung Lee, Development status of reactor physics code suite in UNIST, in: 11st International Conference of the Croatian Nuclear Society, Zadar, Croatia, June 5-8, 2016, Croatian Nuclear Society, 2016.
[16] Hanjoo Kim, Jinsu Park, Jiwon Choe, Jiankai Yu, Deokjung Lee, Multi-physics Coupled Reactor Core Analysis System of RAST-K2.0 with CTF and FRAPCON, in: KNS Spring Meeting, Jeju, Korea, May 16–18, 2018.
[17] Sooyung Choi, Chang Ho Lee, DeokjunG Lee, Resonance treatment using pin-based pointwise energy slowing-down method, J. Comp. Phys. 330 (2017) 134–155.
[18] Maria Pusa, Rational approximation to the matrix exponential in burnup calculations, Nucl. Sci.. Eng. 169 (2011) 155–167.
[19] Jinsu Park, Wonkyeong Kim, Sooyoung Choi, Hyunsuk Lee, Deokjung Lee, Comparative analysis of VERA depletion problems, in: KNS Fall Meeting, Gyeongju, Korea, October 26–28, 2016.
[20] Sooyoung Choi, Pin-based Pointwise Energy Slowing-down Method for Resonance Self-Shielding Calculation, Doctoral Thesis, UNIST, 2017.
[21] Bamidele Ebiwonjumi, Sooyoung Choi, Matthieu Lemaire, Deokjung Lee, Ho Cheol Shin, Experimental Validation of STREAM for Spent Nuclear Fuel Applications, RPHA17, Chengdu, Sichuan, China, August 24–25, 2017.
[22] Hyun Chul Lee, Unified nodal method for static and Transient Analysis of Power Reactor, Thesis (doctoral), Seoul National University, 2001, http://hdl.handle.net/10371/34547.
[23] Z. Weiss, A consistent definition of the number density of pseudo-isotopes, Ann. Nucl. Energy. 17 (3) (1990) 153.
[24] T. Bahadir, S.O. Lindahl, S.P. Palmtag, SIMULATE-4 Multigroup Nodal Code With Microscopic Depletion Model, Mathematics and Computation, Supercomputing, Reactor Physics and Nuclear and Biological Applications, Palais des Papes, Avignon, France, 2005. Sept 12-15, 2005, on CD-ROM, ANS LaGrange Park, IL.
[25] Jinsu Park, Minyong Park, Jiwon Choe, Peng Zhang, Jaerim Jang, Deokjung Lee, Development Status of Dynamic Reactor Nodal Computational Code RAST-K v2.0, RPHA17, Chengdu, Sichuan, China, August 24–25, 2017.
[26] Y.S. Jung, C.B. Shim, C.H. Lim, H.G. Joo, Practical numerical reactor employing direct whole core neutron transport and subchannel thermal/hydraulic solvers, Ann. Nucl. Energ. 62 (2013) 357–374. https://www.sciencedirect.com/science/article/pii/S0306454913003344.
[27] KNF-S1ICD-10004 Rev. 0, The Nuclear Design Report for Shin-Kori Nuclear Power Plant Unit 1 Cycle 1, Korea Nuclear Fuel Company, Ltd, February 2010.
[28] KNF-U4C7–06017 Rev. 0, The Nuclear Design Report for Ulchin Nuclear Power Plant Unit 4 Cycle 7, Korea Nuclear Fuel Company, Ltd, June 2006.
[29] KNF-S3ICD-12034 Rev. 0, The Nuclear Design Report for Shin-Kori Nuclear Power Plant Unit 3 Cycle 1, KEPCO Nuclear Fuel Company, Ltd., October 2012.
[30] KNF-K3C19–08015, The Nuclear Design and Core Physics Characteristics of the Kori Nuclear Power Plant Unit 3 Cycle 19, Korea Nuclear Fuel Company, Ltd., May 2008.
[31] The Nuclear Design Report for Yonggwang Nuclear Power Plant Unit 1 Cycle 19, KNF-Y1C19–09008, Korea Nuclear Fuel Company, Ltd.
[32] Woonghee Lee, Sooyoung Choi, Bamidele Ebiwonjumi, Matthieu Lemaire, Deokjung Lee, Implementation of On-The-Fly Energy Release per Fission Model in STREAM, RPHA17, Chengdu, Sichuan, China, August 24–25, 2017.
[33] Deokjung Lee, Joel Rhodes, Kord Smith, Quadratic depletion model for gadolinium isotopes in CASMO-5, Nucl. Sci.. Eng. 174 (2013) 79–86. https://doi.org/10.13182/NSE12-20.
[34] Deokjung Lee, Kord Smith, Joel Rhodes, The impact of U-238 resonance elastic scattering approximations on thermal reactor doppler reactivity, Annal. Nucl. Energy 36 (3) (2009) 274–280. https://doi.org/10.1016/j.anucene.2008.11.026.
[35] Kord S. Smith, Nodal Diffusion Methods: Understing Numerous Unpublished Details, PHYSOR2016, Sun Valley, ID, USA, May 1–5, 2016.
[36] K.J. Geelhood, W.G. Luscher, P.A. Raynaud, I.E. Porter, FRAPCON-4.0: a Computer Code for the Calculation of Steady-state, Thermal-Mechanical Behavior of Oxide Fuel Rods for High Burnup, Vol. 1, Pacific Northwest National Laboratory, Richland, WA, 2015. PNNL-19417, Rev. 2.
[37] K.J. Geelhood, W.G. Luscher, C.E. Beyer, FRAPCON-4.0: Integral assessment, Vol. 2, Pacific Northwest National Laboratory, 2015. PNNL-19418, Rev. 2.
[38] Tung Dong, Cao Nguyen, Hyunsuk Lee, Jiwon Choe, Ho Cheol Shin, Hwan Soo Lee, Deokjung Lee, LPPT Analysis of APR1400 Reactor Core by UNIST Monte Carlo Code MCS, RPHA17, Chengdu, Sichuan, China, August 24–25, 2017.
[39] Pre-Operational Inspection Report of Shin-Kori Nuclear Power Plant Unit 3 (Initial Fuel Load and Startup Test, Vol. 2, Korea Institute of Nuclear Safety, 2016. KINS/AR-1008, http://nsic.nssc.go.kr/dta/reguResultView.do?seq=882.